Application of Nanofiltration for Rare Earth Elements Recovery from Coal Fly Ash Leachate: Performance and Cost Evaluation

Borte Kose Mutlu[1], Beatrice Cantoni[2], Andrea Turolla[2], Manuela Antonelli[2], Heileen Hsu-Kim[1], Mark R. Wiesner[1,*]

[1] *Duke University, Department of Civil and Environmental Engineering, Pratt School of Engineering, 27708 Durham, North Carolina, United States*

[2] *Politecnico Milano, Department of Civil and Environmental Engineering (DICA) - Environmental Section, Piazza Leonardo da Vinci 32, 20133 Milano, Italy*

Abstract This work evaluated nanofiltration (NF) as a potential step in the recovery process of Rare Earth Elements (REEs) from leachates of coal combustion fly ashes. A pre-treatment step, by pH adjustment and microfiltration (MF), has been studied to separate REEs by major elements. The individual and combined effects of applied pressure (12-24 bar) and NF feed acidity (pH 1.5-3.5) on rejection of six critical REEs and permeate flux have been investigated via response surface methodology (RSM). The resulting model equations were used to develop a cost model for the recovery chain, in order to select the optimum NF operating conditions. The optimization of the REE recovery chain, including pre-treatment and NF, was done with respect to the objective of maximizing the difference between NF concentrate economic value and treatment cost. NF with an appropriate MF pre-treatment has been effective in concentrating REEs from fly ash leachate, reaching the maximum potential gain at the optimum operating conditions of 12 bar and pH 3.5.

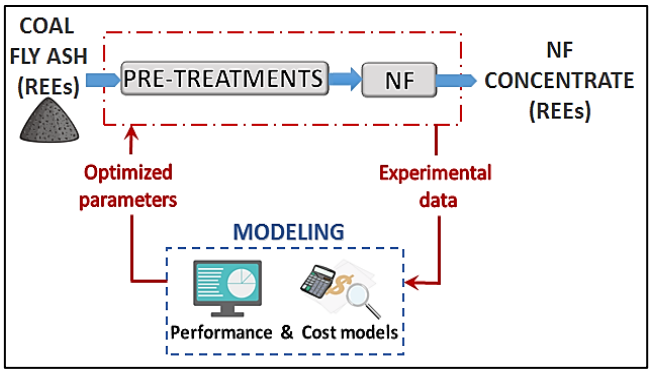

Graphical Abstract

Keywords Coal Combustion Residues; Critical Elements; Membrane Technology; Response Surface Methodology; Cost Model.

List of Abbreviations Analysis of Variance (ANOVA); Central Composite Face-centered (CCF); Design of Experiment (DoE), Inductively Coupled Plasma-Mass Spectrometry (ICP-MS); Iso-electric Point (IEP); Microfiltration (MF); Mixed Cellulose Ester (MCE); Molecular Weight Cut-off (MWCO); Nanofiltration (NF); Polycarbonate (PC); Polyethersulfone (PES); Rare Earth Elements (REEs); Response Surface Methodology (RSM); Spiral Wound (SW); Supporting Information (SI); Thin Film Composite (TFC); Zeta Potential (ZP).

1. INTRODUCTION

The Rare Earth Elements (REEs) are a group of 16 elements consisting of the 14 stable lanthanides plus scandium and yttrium [1]. REEs are strategic materials in a wide range of applications including key technologies related to transportation, communication and clean energy supply. There is uncertainty surrounding the availability of REEs due to the increasing demand for modern technologies and a geopolitically limited number of suppliers. China currently supplies more than 86% of global REEs production, and in recent years has steadily increased export taxes, while restricting export quotas [2]. The U.S. Department of Energy

has underscored the need for alternative sources of REEs, especially for critical elements such as Nd, Eu, Tb, Dy, Y, and Er [3].

Fly ash originating from coal combustion at power plants has been investigated as a potential alternative source of REEs due to their enrichment in fly ash, and the economic and environmental issues generated by ash disposal [4]. Previous studies reported that many coal deposits contain high levels of REEs, and the respective ashes are also rich in REEs [4–8]. However, these past research efforts have largely focused on quantifying the total REE content in coal fly ash (inter alia, [8]), while the performance and feasibility of recovery processes are still scarcely studied. Part of the challenge lies in the complex mixtures generated when REEs are leached from fly ash particles into solution. Strong acids such as nitric acid (HNO_3) can be relatively efficient in leaching REEs from coal fly ash (>60% for fly ashes generated from western U.S. coals); however, this leachate comprises very low pH and a mixture of major elements such as Ca, Si, Al, Fe, Na, and Mg that are 10^2 to 10^4 times greater in concentration than individual REEs [4].

Highlighting the lack of economical alternatives among conventional technologies [9], several recent works have considered REE recovery from different sources through alternative and innovative techniques, using a variety of biological and chemical processes. For example, biosorption with yeast cells, fungus, algae and plant cells such as *Candida utilis*, *Schizophyllum commune*, *Sargassum* spp. and *Platanus orientalis* can bioconcentrate REEs from dilute solutions [10–14]. However, biosorption capacity tends to require near neutral or mildly acidic pH values, limiting the application of biosorption from acid solutions that are required to leach REEs from fly ash [10,14]. The most common chemical techniques for REEs recovery are ion exchange [15,16], adsorption using special adsorbents like layered double hydroxide [17], gel particles of alginic acid [18] or activated carbon [19], and chemical precipitation [20,21]. Unfortunately, chemical methods are usually characterized by

high operating and environmental costs due to the high amounts of chemical reagents required [22].

To avoid the impacts resulting by the high amounts of chemical reagents, membrane processes have been used to separate REEs in dilute solution with low operating costs. Shimizu et al. (1992) [23] patented a process including reverse osmosis to concentrate solutions having high flow rates and low REE concentrations. Supported liquid membranes with chelating agents, such as di(2-ethylhexyl)phosphoric acid and diethylenetriaminepentaacetic acid, have been used to concentrate neodymium with efficiencies up to about 93% [24,25]. Wen et al. (1999) [26] indicated that an innovative hollow fiber membrane, composed of 8-hydroxyquinoline immobilized polyacrylonitrile, can concentrate REEs at least 300 times their feed concentration. Murthy and Gaikwad (2013) [27] demonstrated that nanofiltration (NF) is an effective process for the separation of praseodymium(III) from acid aqueous solutions, with 89% separation efficiency.

Thanks to lower energy consumption, compared to RO, and for the absence of chelating agents, compared to supported liquid membranes, NF has been identified as a promising and sustainable technology for the removal of multivalent solutes at low concentrations from complex process streams [28]. In the case of coal fly ash leachates, NF would be useful for separating major monovalent ions (e.g., NO_3^-, Cl^-, Na^+) from trivalent REEs as part of a multistep process for REE purification. The main criteria for assessing NF performance can be roughly reduced to those of retention of the solutes and maintenance of permeate flux through the membrane [29]. Applied pressure tends to increase membrane permeate flux, while increasing the transport of REEs and foulants to the membrane. The effect of transmembrane pressure on ion rejection is highly dependent on the characteristics of the solution to be treated [30–32]. The feed solution pH has a significant effect on rejection and flux maintenance as it alters the charge of functional groups on the membrane and may affect

charge and speciation of solute [33,34]. By reducing the pH, the amount of positively charged functional groups increases, resulting in a positive zeta potential (ZP) that may increase retention of cationic compounds (metal ions) [35]. Thus, a challenge in applying NF to complex streams includes finding the optimal combinations of operating conditions for the separation of target molecules.

While many works have been published on NF performance, there are relatively few publications addressing the design and optimization of the process from an economic standpoint. In the case of resource recovery, such as REE recovery, costs can be directly compared with product economic value dictated by the market for the recovered material. In addition to market benefits, REEs recovery from coal fly ash is a promising strategy to avoid two main environmental impacts associated, on one hand, with the toxicity of the initial material, and, on the other hand, with the REEs mines extraction activities.

Despite the considerable progress in transport modeling of membrane processes, at present, it is still difficult to accurately predict the performance of NF membranes used to treat complex mixtures. Instead, performance estimates for NF applications involving feed flows more complex that seawater or brines are still best derived by piloting the process [30]. In fact, since the economics of membrane filtration have been shown to be largely dependent on permeate flux [36,37], an accurate estimation of case-specific permeate fluxes, necessarily obtained from pilot studies, is usually a needed step for estimating costs [38,39].

The aim of this study was to experimentally identify the optimum NF configuration for concentrating REEs from leachates of coal fly ashes and to assess its costs if membrane separation was one of multiple steps used in REE purification. While NF membranes are expected to concentrate trivalent REEs in acidic solutions and separate monovalent ions, NF would not necessarily separate REEs from other major elements present in the coal fly ash leachates (e.g. Al, Si, Fe). Thus, a pre-NF step comprised of pH adjustment and

microfiltration (MF) was also investigated and the product of this pre-treatment was used to study the effects of applied pressure and pH on the NF concentration step. All tests were performed on a simulation of a coal ash leachate. Synthetic leachates (rather than actual leachate of fly ash) were used mainly to enable reproducible membrane testing of a consistent feed leachate that has the potential to precipitate secondary minerals over long storage times (weeks and months). Finally, a cost model was used to determine the optimum NF operating conditions.

2. MATERIALS AND METHODS

2.1 Reagents. 1000±5 μg L^{-1} standard solutions of Tb, Nd, Y, Eu, Er, and Dy containing 7% HNO_3 (v/v) were purchased from Inorganic Ventures (USA) and used as source of REEs. Nitrate salts, i.e. $NaNO_3$, $Mg(NO_3)_2{\cdot}6H_2O$, $Ca(NO_3)_2{\cdot}4H_2O$, $Al(NO_3)_3{\cdot}9H_2O$, $Na_2Si(NO_3)_3{\cdot}9H_2O$, and $Fe(NO_3)_3{\cdot}9H_2O$, were purchased from Sigma-Aldrich (USA). pH adjustments were done with HNO_3 (15.7 M, 99.999% purity for trace metal analysis) and NaOH (5 N, prepared from powder, reagent grade, 99.97% purity) supplied from Sigma-Aldrich (USA). All experiments were carried out using doubly deionized water (Barnstead NanoPure (NP)).

2.2 Membranes. Four different MF and NF membranes were used for the pre-treatment and concentration experiments, respectively. These membranes have been selected according to their suitability to operate at low pH and to their applications reported in the manufacturer datasheets and in scientific literature [31,40,41]. MF membranes are abbreviated to ‘MF(pore size)’ hereafter. The technical properties of the membranes, which were supplied by manufacturers, are presented in Table 1.

Table 1. Technical properties of MF and NF membranes used in the experiments, based on suppliers' datasheets.

Membrane model	Class	Supplier	Membrane material *	Pore size / MWCO	Permeability ($L/m^2/h/bar$) [α]	Salt Rej. (%)	P_{max} (bar)	pH
GPWP04700	MF	Merck Millipore	PES	0.22 µm	13.044	-	<1.4	N/A
HAWP04700	MF	Merck Millipore	MCE	0.45 µm	52.176	-	<1.8	N/A
AAWP04700	MF	Merck Millipore	PES	0.80 µm	101.736	-	<0.9	N/A
WHA111110	MF	Whatman Nuclepore	PC	1.00 µm	132.000	-	<0.96	N/A
NP010	NF	Microdyn-Nadir	PES	1000 Da	5-10	35-75[β]	40	0-14
NP030	NF	Microdyn-Nadir	PES	500 Da	1-1.8	80-95 [β]	40	0-14
DK	NF	GE W&P Tech.	TFC	150-300 Da	5.5±25%	96[γ]	40	1-10
Duracid	NF	GE W&P Tech.	TFC	150-200 Da	1.1-2.1	98 [γ]	60	0-9

** PES: Polyethersulfone; MCE: Mixed Cellulose Ester; PC: Polycarbonate; TFC: Thin Film Composite*

[α] *The permeability of MF membranes was calculated using water flow rate data (mL/min/cm^2 at 690 mbar)*

[β] *Tested salt: Na_2SO_4*

[γ] *Tested salt: $MgSO_4$*

2.3 Characteristics of Synthetic Leachate. Separation experiments were performed on a simulated fly ash leachate that was based on major elements and REEs concentration measurements of HNO_3 leachates of four coal combustion residues (fly ash, stoker ash, and pond ash) subjected to alkaline sintering, as reported by Taggart et al. (2016) [4] and described further in Supporting Information Table S1. The four coal combustion residues were obtained from power plants located in South Carolina and Kentucky and were burning coals from the central Appalachian Basin. This simulated leachate comprised six REEs (Y^{3+}, Nd^{3+}, Dy^{3+}, Er^{3+}, Eu^{3+}, Tb^{3+}) at 0.15 mg L^{-1} each and selected for their criticality. The synthetic leachate also contained major elements Mg^{2+}, Ca^{2+}, Fe^{3+}, Al^{3+}, Si^{4+}, and Na^{+} (ranging in concentration from 10 to 6300 mg L^{-1}) dissolved into water from their respective nitrate salts or HNO_3-acifidied stock solutions. The pH of the synthetic leachate was adjusted

to 1.0 by using HNO_3 (1%, v/v). The synthetic leachate was prepared daily to minimize precipitation of secondary mineral particles.

2.4 Pre-treatment of Leachate by pH Adjustment, Precipitation and MF. The influence of the pH of feed solution was tested by adding dissolved NaOH to the simulated ash leachate solution and targeting pH values from 1.5 to 5.0. The samples were held static and the supernatant was immediately (e.g. within 5 minutes) collected for analysis of individual REEs and major elements. A subset of pH-adjusted samples (pH 3.3 to 4.3) was filtered by various MF membranes to test for the importance of nominal pore size for REE and major cation recovery. Samples of 5 mL were filtered immediately after pH adjustment by MF disc filters (Table 1) placed on a glass vacuum filtration apparatus (VWR 28144, USA). MF membranes were dried at 105^{o}C for 2 h and weighed to measure the mass of collected chemical precipitates while the MF filtrate was collected for analysis of individual REEs and major elements. The precipitation time was tested by repeating the procedure after 20, 40, 60 and 90 minutes from pH adjustment using MF(0.45) membrane. All tests were repeated twice.

2.5 Characterization of NF Membranes. Pure water permeability tests were conducted using a cross-flow flat sheet filtration system (Figure S1). The membrane cell, SEPA CF II (GE Osmonics, USA), had an active membrane area of 135 cm^2. Prior to each test, the system was operated in circulation mode and the membrane was conditioned with NP water for 2 h at a constant pressure of 25 bar. Tests were conducted at three applied pressures (12, 18 and 24 bar) for each NF membrane at room temperature (25 °C). After the permeate flux stabilized, permeate mass was measured by weighing with a balance (OHAUS Adventurer,

0.01 g precision, USA) and Equations (1) and (2) were used for the permeate flux calculation. NF membrane permeability was calculated by the Spiegler and Kedem equation (Equation 3).

$$V_p = \frac{m_p}{\rho} \quad (1)$$

$$J_p = \frac{V_p}{A\,\Delta t} \quad (2)$$

$$J_p = L_p\,(\Delta P - \sigma\,\Delta\pi) \quad (3)$$

where V_p is the volume of permeate (L), m_p is the mass of permeate (g), ρ is the density of permeate (g cm^{-3}), J_p is the permeate flux (L m^{-2} h^{-1}), A is the effective membrane area (m^2), Δt is the sampling time (h), ΔP is the applied pressure (bar), σ is the reflection coefficient, Δπ is the osmotic pressure difference (bar) assumed as zero when water permeability was calculated, and L_p is the solution hydraulic permeability (L m^{-2} h^{-1} bar^{-1}).

The ZP was determined through the tangential streaming potential method based on the measurement of the increase of electric potential as an electrolyte solution (0.1 M KCl at 25°C) passed between two membranes oriented with their active layers facing each other under the defined applied pressure gradients. The pH of electrolyte solution was adjusted between 2.9 and 11.5. The ZP was calculated according to Equation 4.

$$\zeta = \frac{\nu_p\,\lambda_0\,\eta}{\varepsilon_0\,\varepsilon_b} \quad (4)$$

where ζ is the ZP (V), ν_p is the streaming potential (V Pa^{-1}), λ_0 is the solution average conductivity (S m^{-1}), η is the electrolyte dynamic viscosity (Pa s), ε_0 is the vacuum permittivity (F m^{-1}) and ε is the dielectric constant of the electrolyte.

2.6 Experimental Plan for NF Concentration Tests. The DoE methodology was applied [42] entailed the following. First, a two-level full factorial design was prepared, as reported in Table 2. Accordingly, 4 tests were performed on the synthetic pre-treated leachate

at different pH and pressures using four NF membranes. A total of 16 experiments was carried out. Since the MF permeate pH is 3.5, to simulate a condition of no additional pH adjustment, one pH level was set to 3.5. Moreover, since DK membrane acceptable minimum pH is 1.0, 1.5 was determined as the minimum pH level to be tested in order not to damage the membranes. As for the pressure, among the most commonly evaluated range in nanofiltration experiments in literature (5-40 bar) [31,32,43], the tested levels have been selected equal to 12 bar, to achieve a measurable pre-treated leachate permeation through the membranes, and 24 bar, to avoid laboratory safety risks due to the filtration system acceptable pressure. Then, the experimental dataset was expanded by a central composite face-centered (CCF) design, defined according to the Response Surface Methodology (RSM) (Table 2). Accordingly, a set of 9 experiments was performed on the synthetic pre-treated leachate using DK membrane. A total of 26 experiments (4 from the two-level full factorial) was carried out. The number of replicates for each experiment is detailed in Table 2.

Table 2. Experimental plan for Design of Experiment (DoE) schemes that first enatiled a two-level full factorial design followed by a central composite face-centered (CCF) design.

Design	**Experiment #**	**Membrane**	**Experimental Variables (Factors)**		**Replicates**
			Pressure (bar)	**Feed pH**	
Two-level full factorial design	1	NP010, NP030, DK, Duracid	12	1.5	1 per membrane
	2		12	3.5	1 per membrane
	3		24	1.5	1 per membrane
	4		24	3.5	1 per membrane
CCF design	1*	DK	12	1.5	2
	2	DK	12	2.5	2
	3*	DK	12	3.5	2
	4	DK	18	1.5	2
	5	DK	18	2.5	10
	6	DK	18	3.5	2
	7*	DK	24	1.5	2
	8	DK	24	2.5	2
	9*	DK	24	3.5	2

** One repetition of the experiment from the two-level full factorial design.*

Experiments were carried out with the same system and compaction procedure used for water permeability tests. The initial feed volume was 2 L and the temperature during the operation was 25±1°C. The feed pump was set at a flow rate Q_F = 0.384 L h^{-1}. Both concentrate and permeate have been recirculated in the feed tank, not to vary the feed solution composition. After the permeate flux stabilized (in about 1 h), concentrate and permeate flow rates have been measured and permeate flux calculated as explained previously. 3 mL of concentrate and permeate were collected for elemental analysis. The membrane rejection for each element, *i*, has been calculated with Equation (5).

$$Rej_i = (1 - \frac{C_{p,i}}{C_{f,i}}) \cdot 100 \quad (5)$$

where Rej_i is the rejection of element *i* (%), $C_{p,i}$ is the concentration of element *i* in the permeate (mg L^{-1}) and $C_{f,i}$ is the concentration of element *i* in the feed (mg L^{-1}). A one-way analysis of variance (ANOVA) has been performed on rejection data.

2.7 Analytical Methods. pH was measured by Fisher Scientific probe (XL Series, USA). Elemental analysis was performed using inductively coupled plasma mass spectrometry (Agilent 7900 ICP-MS, USA) operated under helium reaction gas mode to minimize polyatomic interferences for trace elements. Standard solutions (Inorganic Ventures, USA) were used as internal standards for calibration as recommended by the manufacturer and the correlation coefficient was higher than 0.9995 for all measurements. Standard and samples of ICP-MS were acidified using 2% HNO_3 (v/v), while all measurements were repeated three times. ZP was determined using an electrokinetic analyzer (Anton Paar Surpass, Austria).

2.8 Cost Analysis. Previously developed cost models for membrane systems [44,45] were adapted in this work to estimate capital and operating costs for a full-scale NF facility. The cost model was applied using experimental estimates of permeate flux and REE rejection as

well as assumptions on chemical use corresponding to those used in experiments. The operating costs due to base and acid dosage are summarized in SI (Table S2). MF has been considered as a pre-treatment step, while spiral wound (SW) configuration has been selected as the most reliable for full-scale NF. Capital costs due to membranes, pipes, valves, instruments, controls, tanks, frames, miscellaneous equipment and facilities and pumps have been considered. Capital cost estimates for MF and SW-NF steps from Sethi et al. (2001) [45] have been updated, to consider the equipment cost increase from 2001 to 2015, with the Chemical Engineering Plant Cost Index (CEPCI), according to Equation (6):

$$\mathrm{Cost}_{i(2015)} = \frac{\mathrm{CEPCI}_{i(2015)}}{CEPCI_{i(2001)}}\ \mathrm{Cost}_{i(2001)} \qquad (6)$$

The CEPCI values of the filtration system equipment are reported in SI (Table S3). Operating costs for membrane replacement, energy consumption, chemical dosage and REEs-poor stream disposal have been considered for MF and NF steps. MF full-scale configuration includes: concentrate recirculation, fast-flush and back-flush, concentrate disposal. SW-NF full-scale configuration does not include: concentrate recirculation, fast-flush and back-flush. NF permeate stream is sent to disposal. The list of the parameters used in the cost model is reported in SI (Table S4).

Knowing the NF concentrate contents of each REE (including scandium that has not been experimented), the NF concentrate economic value was estimated according to the 2016 sell prices of REEs (Table S5).

3. RESULTS AND DISCUSSION

3.1 Pre-treatment of Leachate. Based on the results of a first set of precipitation experiments, not reported in this paper, the pre-treatment experiments testing for settling time and pore size of MF membranes were carried out in the pH range 3.3-4.3. The optimum pore

size was determined as the largest pore size providing the complete rejection of precipitated particles, thereby maximizing the permeate flux. The mass of rejected precipitates increased with increasing pH and decreasing pore size (Table S6). Nominal pore sizes of 0.45 µm and 0.22 µm produced no significant difference in rejection while smaller mass of particles was captured by membranes with larger nominal pore size. Therefore, the 0.45 µm membrane was selected for further experimentation.

The optimum precipitation time was determined as the time to maximize the removal efficiency of competitive elements and minimize the loss of REEs. The fraction of major elements and REEs remaining in solution was relatively constant with time intervals from <5 min to 90 min (Figure S2). Because major trivalent co-ion precipitation occurred instantaneously (i.e. within 5 minutes), an in-line precipitation process was selected for the cost analysis.

The pH of the leachate solution for the MF filtration step was another important variable in determining removal and recoveries of major cations and REEs (Figure S3). At pH 4.0 REE concentrations in the MF permeate (about 88% of the feed concentration) were observed to be higher than in solutions adjusted to pH values above 4.3 (about 75% of REEs recovered). This REEs loss was expected to be due to their sorption on solid phase precipitates formed by the major elements. REE purity increased as the pH increased from 3.8 to 4.0 due to the additional loss of iron, silicon and aluminum. Thus pH 4.0 appeared to be the optimal value to maximize REE concentration in solution while also removing substantial amounts of Fe, Si, and Al (removal of approximately 98%, 41%, and 50%, respectively). At pH 4.0, no changes were observed for dissolved sodium, calcium and magnesium concentrations (Table S7). The precipitation and MF processes resulted in a pH shift from the adjusted optimum value 4.0 to the final pre-treated value of about 3.5.

3.2 Characterization of NF Membranes. NF membranes were tested for their ability to further concentrate REEs in the process. First, the surface properties of the four NF membranes were assessed by measuring the streaming potential, expressed as ZP.

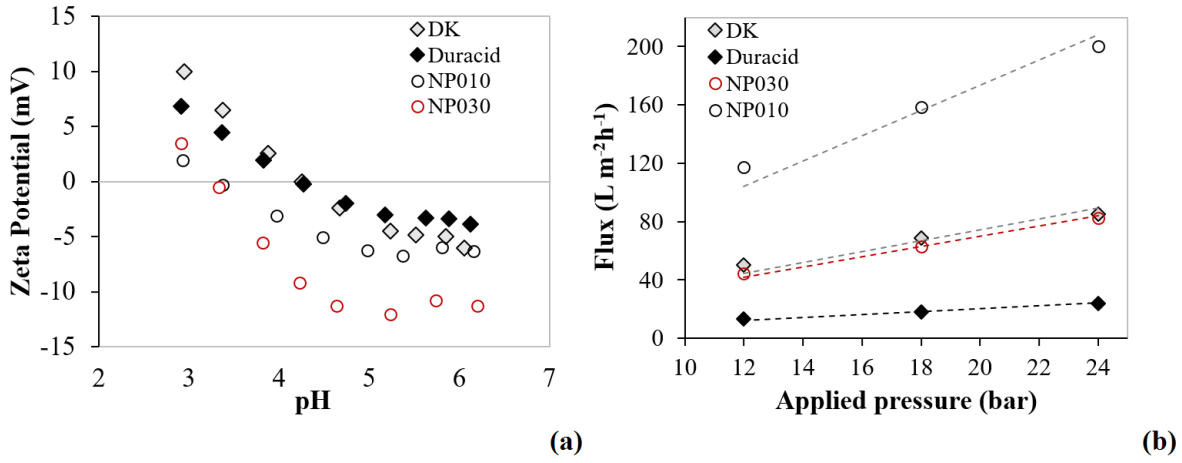

Figure 1. Characteristics of the tested NF membranes: (a) ZP as a function of the pH of electrolyte (KCl, 0.1 M), (b) water permeate flux as a function of the applied pressure.

The results demonstrated that the two PES membranes, NP010 and NP030, have similar iso-electric points (IEP) at pH 3.3 and 3.2, respectively (Figure 1a). These results suggest that feed solutions with this pH value or lower should favor rejection of REEs. The other two TFC membranes, DK and Duracid, have similar IEPs at pH 4.2 and 4.3, respectively. By the same logic, these NF membranes would be anticipated to reject REEs throughout the range of pH values studied for the synthetic fly ash leachate feed. Overall, the ZP data indicate that the lowest rejection of REEs is expected for NP010 and the highest for DK.

A linear dependence of permeate flux on the applied pressure was observed (Figure 1b), characterized by the intercept in the axis origin and R^2 values higher than 0.91 for all membranes. The values of water permeability (Lp) for each membrane are detailed in SI (Table S8). NP010 had the highest NP water permeability, about eight times that of Duracid.

DK and NP030 were characterized by intermediate values of Lp between Duracid and NP010, being DK slightly more permeable than NP030.

3.3 NF Concentration of Leachate

3.3.1 Selection of NF Membrane. The permeability, Lp', of NF membranes to pre-treated synthetic leachates tended to be the highest for the NP010 membrane and the lowest for Duracid membrane (Table S8). Permeability was affected by the nominal Molecular Weight Cut-off (MWCO) but also decreased with increasing membrane thickness and with decreasing porosity, all factors that are related to the membrane material [46]. These properties of the membranes may explain the higher leachate permeability for PES compared with the TFC membranes. Additional resistance to permeation could be provided by rejected ions on the membrane surface and inside the pores [43]. REE rejection was less than 15% for NP010 and NP030 membranes at pH 1.5 and 3.5 and applied pressures of 12 and 24 bar (Table S9). The relatively high permeability of REEs for all test conditions was probably due to the combined effect of high MWCO and low positive charge, respectively affecting the sieving and Donnan potential rejection mechanisms. In contrast, the DK membrane exhibited high rejections (>90%) under all operating conditions while the REE rejection was 80-90% for Duracid membrane, possibly due to the higher ZP for the DK membrane. Based on these results, the DK was selected for further optimization for REE recovery.

3.3.2 Optimization of NF concentration step. To evaluate the presence of differing behaviors among REEs in rejection on NF membranes at different applied pressures and pH values, a one-way ANOVA was performed on the experimental data to test the null hypothesis of equal distribution of REE rejections. Since the F-value was equal to 0.135, lower than the F-critical (2.303), the null hypothesis of equal distribution was accepted.

Consequently, one unique CCF design was carried out for investigating the influence of pressure and pH on the average REE rejection. The results (Table S10) demonstrated that varying the rejection of REEs were in the range 92.8-99.3% and depended on the combination of operating conditions. The full quadratic stepwise analysis, including all linear, quadratic and interaction effects of pressure and pH on the response, was used to select significant terms, applying a significance level of 0.05. ANOVA results are shown in SI (Table S11). The analysis yielded a model (Equation 7) for rejection as a function of the first order effects of pressure and pH, as well as an interaction effect between the two factors. The parameter with the highest effect contribution on REEs rejection was pH (84.98%), compared to the linear effect of pressure (10.01%) and their interaction (1.01%).

$$Rej_{REE} = 95.11 + 1.512 \cdot pH - 0.285 \cdot pressure + 0.056 \cdot pH \cdot pressure \qquad (7)$$

The R^2, the adjusted R^2 and the predicted R^2 for this model and the data are respectively 0.9601, 0.9546 and 0.9483 (Figure 2).

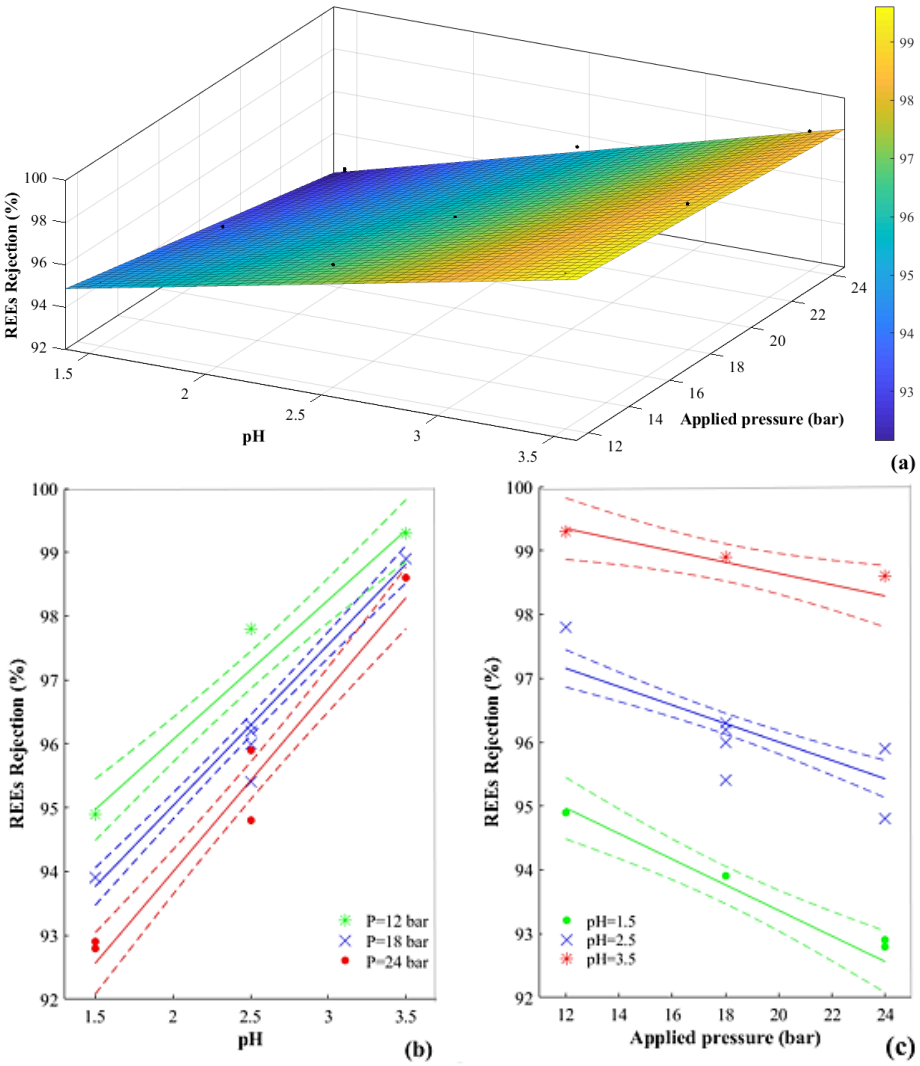

Figure 2. REE rejection for the DK membrane according to the CCF design: (a) 3D trend as a function of both pH and applied pressure; 2D trend as a function of pH (b) and applied pressure (c) (dashed lines report the 95% interval of confidence).

The decrease in REE rejection with pressure is probably due to the prevailing influence of surface forces over drag forces within pores at low pressure, resulting in higher rejection [32]. In contrast with anticipated trends of high rejection for condition that favor a positively charged membrane, REE rejection increased with pH and the associated drop in ZP (Figure 1a). The lowest REE rejection occurred at a pH value of 1.5, at which the feed solution had the highest ionic concentration due to the addition of HNO_3 for the pH adjustment. Ong et al. (2002) [47] suggested that an increase in ionic concentration of feed solution can cause an

increase in ionic concentration on membrane surface, therefore reducing the Donnan potential, and shielding counter-ions from membrane repulsion with a resulting increase in ion permeation. The interaction effect of pH and pressure on REE rejection is positive, meaning that the effect of pH on REE rejection increases with the pressure. The model predicts the maximum REE rejection at minimum pressure (12 bar) and maximum pH (3.5). In addition, the expected separation of monovalent ions from REEs has been accomplished during the NF tests of this study. In fact, while high REEs rejection was achieved, Na+ rejection was lower than 10% meaning that more than 90% of the sodium entering the NF process permeated through the membrane.

The permeate flux of the DK membrane was the second response analyzed by CCF design, and it is reported in SI (Table S10). The permeate flux varied in the range of 16.2-26.8 L m^{-2} h^{-1} depending on the combination of parameters. An analogous procedure for processing data for REE rejection was applied to the permeate flux data. ANOVA results are shown in SI (Table S12). The permeate flux was affected by first order effects of pressure and pH, quadratic effect of pH and the interaction effect between the two factors. The parameter with the highest effect contribution on flux was pressure (76.58%), compared to the linear effect of pH (12.01%), the quadratic effect of pH (7.62%) and factors interaction (1.04%). The resulting permeate flux model as a function of applied pressure and pH is described by Equation (8).

$$\text{Flux} = 0.54 + 8.2 \cdot \text{pH} + 0.85 \cdot \text{Pressure} - 1.616 \cdot \text{pH}^2 - 0.09 \cdot \text{pH} \cdot \text{Pressure} \quad (8)$$

The R^2, the adjusted R^2 and the predicted R^2 were respectively 0.9724, 0.9671 and 0.9515. The experimental measurements are compared with model estimates in Figure 3.

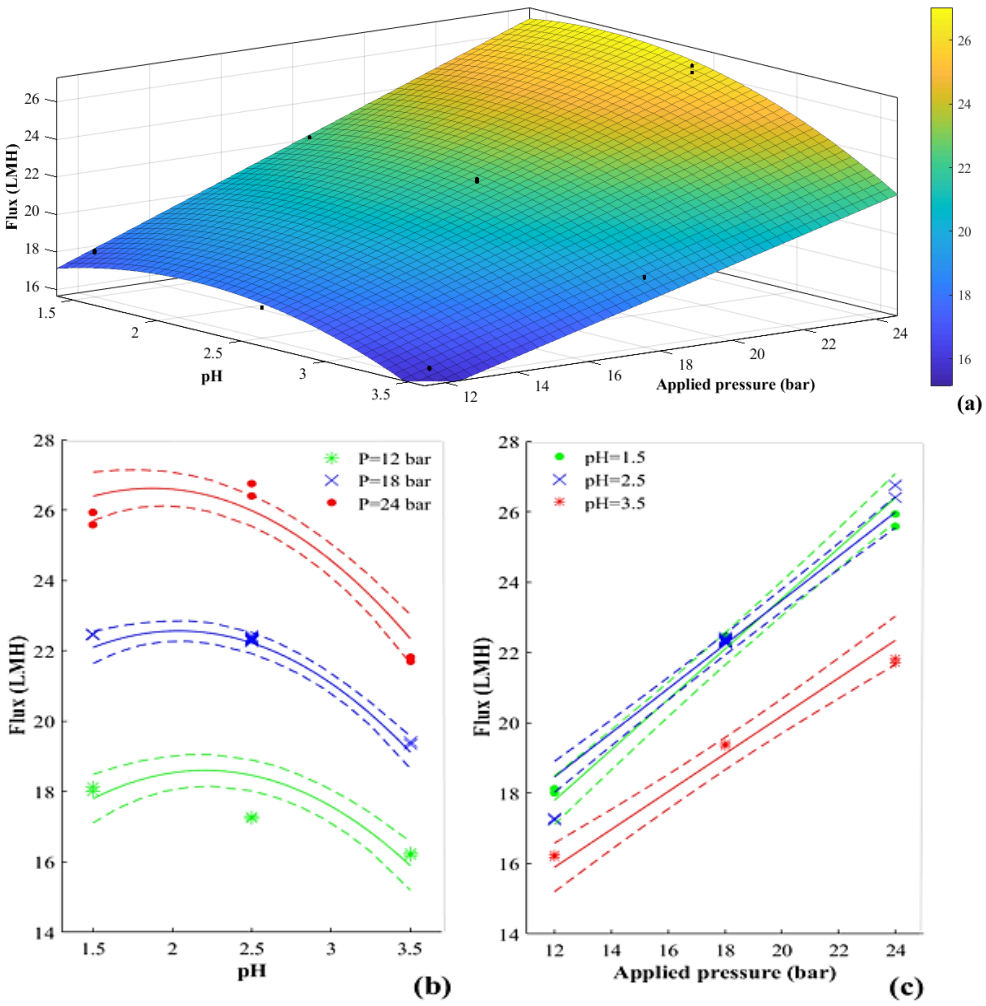

Figure 3. Permeate flux for the DK membrane according to the CCF design: (a) 3D trend as a function of both pH and applied pressure; 2D trend as a function of pH (b) and applied pressure (c) (dashed lines report the 95% interval of confidence).

Permeate flux is linearly proportional to applied pressure, while pH exerts a quadratic concave effect. The dependence on applied pressure is described by the Spiegler and Kedem equation (Equation 3). In this case, where the interaction between pressure and pH has a significant effect on permeate flux, the permeability coefficient is a function of pH according to Equation 9:

$$Lp = 0.85 - 0.09 \cdot pH \quad (9)$$

The pre-treated leachate permeability decreases linearly with pH, in accordance with the negative value of the interaction coefficient. A possible explanation relies in the increase, with the pH, of membrane pores size, also impacting on permeate flux [33]. In addition, the decrease in permeate flux with pH can be attributed to the higher ion rejection. As more ions are rejected, concentration polarization, membrane fouling on the surface and in the pore inlet are expected to reduce permeate flux [43,48]. The maximum permeate flux is predicted by the model at maximum pressure (24 bar) and minimum pH (1.5), contrarily to operating conditions resulting in optimal REE rejection.

3.4 Cost Analysis. Trade-offs between REE rejection and permeate flux will impact overall recovery costs as well as NF concentrate economic value associated with REE yield. The cost model considered these trade-offs and included pH adjustment and MF pre-treatment. Annual amortized capital costs and operating costs ($ $year^{-1}$) were estimated. Specific capital and operating costs ($ kg_{ash}^{-1}) have been calculated normalizing the annual cost to annual mass of coal fly ash entering the recovery plant (8,760,000 kg_{ash} $year^{-1}$). Specific capital and operating costs for each process step as a function of the operating conditions are detailed in Figure 4.

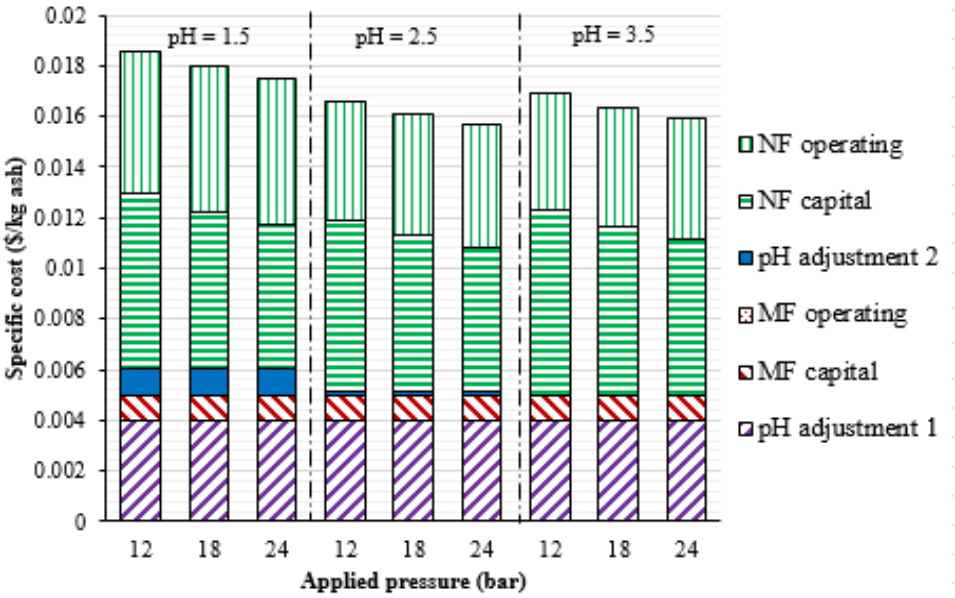

Figure 4. Specific capital and operating costs for the process steps as function of applied pressure and pH.

The total REE concentration specific cost varied from 0.016 to 0.019 \$ kg_{ash}^{-1} depending on the operating conditions. At each value of pH, costs were predicted to decrease with increasing applied pressure due to the decreased membrane area required.

The NF concentrate economic value was estimated according to the REEs content and 2016 sell prices. The specific NF concentrate economic value (\$ kg_{ash}^{-1}) have been calculated normalizing the annual economic value (\$ $year^{-1}$) to the annual mass of coal fly ash entering the recovery plant. The specific economic values for each REE are reported in Table S13 as a function of applied pressure and pH, varying from 0.688 to 0.735 \$ kg_{ash}^{-1}. Scandium economic value corresponds to 97.8% of the total value of the NF concentrate. Since NF concentrate economic values are always one order of magnitude higher than REE concentration costs, NF process remains in the realm of possible REEs recovery technologies. The difference between the NF concentrate economic value and total process costs per kg of coal fly ash is here referred to as potential specific gain. To optimize the operating conditions

of NF concentration process, the potential specific gain was chosen as optimization parameter, reported as a function of applied pressure and pH in Figure 5.

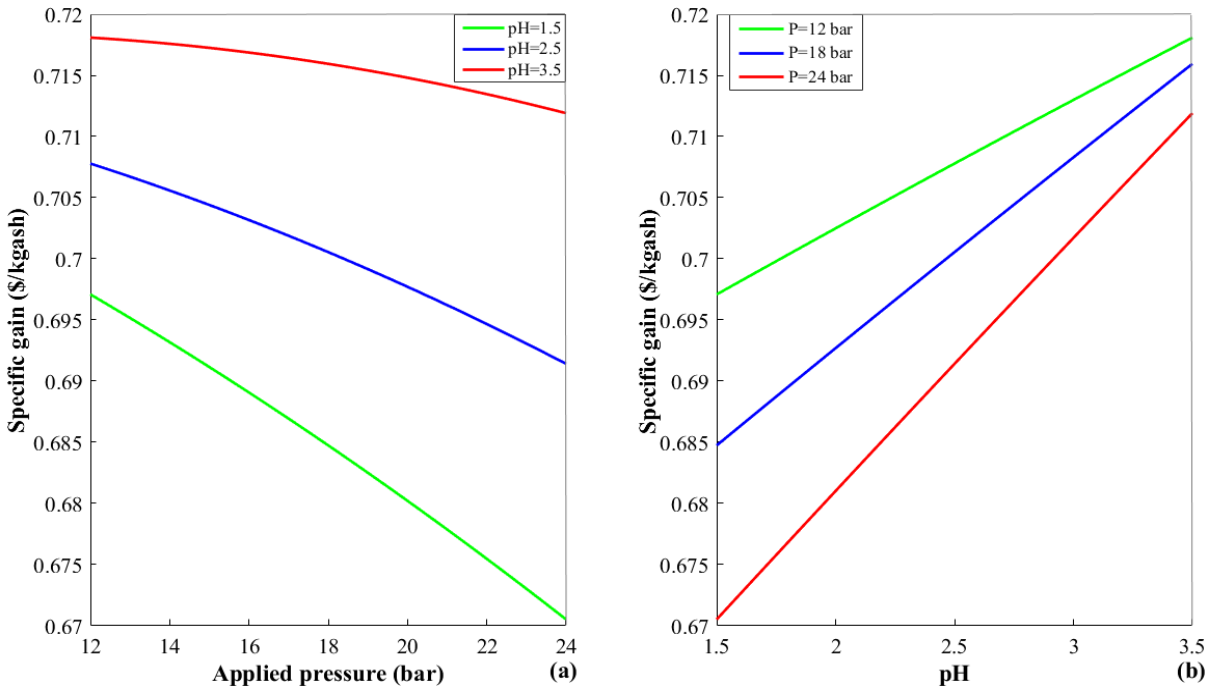

Figure 5. Specific gain calculated with the cost model as a function of applied pressure (a) and pH (b).

The optimal NF operating conditions, maximizing the potential specific gain, are minimum applied pressure, 12 bar, and maximum feed pH, 3.5 (Figure 5). Thus, no second pH adjustment is required in the process line. Furthermore, selecting the minimum pressure we expect to reduce safety and maintenance issues for the NF concentration process.

4. CONCLUSIONS

In conclusion, in addition to the experimental performance analysis, feasibility assessment is also essential in decision making to optimize the REE concentration process. The combination of MF pre-treatment and NF process enables to improve the fly ash leachate stream quality concentrating REEs and partially separating major elements, reaching the

maximum potential gain at the optimum operating conditions of 12 bar and pH 3.5. Recovery studies with real leachates are required to evaluate the fouling mechanism and the effect of feed concentration on the rejection efficiency. Within this regard, it can be mentioned that nanofiltration as an alternative method for REE recovery from fly ashes will have an important potential in the pilot- and real-scale recovery technologies in the future.

AUTHOR INFORMATION

Corresponding Author

*Phone: 1-919-660-5292. E-mail: wiesner@duke.edu

Notes

The authors declare no competing financial interest.

ACKNOWLEDGEMENTS

The research was supported by the U.S. Department of Energy under the Project No. DE-FE0026952 and the U.S. National Science Foundation Environmental Engineering program (CBET-1510965). The financial support for Dr. Borte Kose-Mutlu was provided by TUBITAK 2219-International Postdoctoral Research Fellowship Program. The authors thank Ross Taggart for providing coal fly ash leachate, Prof. Dr. Dincer Topacık National Research Center on Membrane Technologies (MEM-TEK) for ZP measurements, and David Dickerson for supplying NP010 and NP030 membranes.

REFERENCES

[1] S. Wu, L. Wang, L. Zhao, P. Zhang, H. El-Shall, B. Moudgil, X. Huang, L. Zhang, Recovery of rare earth elements from phosphate rock by hydrometallurgical processes – A critical review, Chem. Eng. J. 335 (2018) 774–800.

[2] R.A. Crane, D.J. Sapsford, Sorption and fractionation of rare earth element ions onto nanoscale zerovalent iron particles, Chem. Eng. J. 345 (2018) 126–137.

[3] D. Bauer, D. Diamond, J. Li, D. Sandalow, P. Telleen, B. Wanner, (DOE), Critical Materials Strategy: US Department of Energy, 2010.

[4] R.K. Taggart, J.C. Hower, G.S. Dwyer, H. Hsu-Kim, Trends in the Rare Earth Element Content of U.S.-Based Coal Combustion Fly Ashes, Environ. Sci. Technol. 50 (2016) 5919–5926.

[5] R.B. Finkelman, Trace and Minor Elements in Coal, in: Springer, Boston, MA, 1993: pp. 593–607.

[6] S.M. Mardon, J.C. Hower, Impact of coal properties on coal combustion by-product quality: Examples from a Kentucky power plant, Int. J. Coal Geol. 59 (2004) 153–169.

[7] M.P. Ketris, Y.E. Yudovich, Estimations of Clarkes for Carbonaceous biolithes: World averages for trace element contents in black shales and coals, Int. J. Coal Geol. 78 (2009) 135–148.

[8] V. V. Seredin, S. Dai, Coal deposits as potential alternative sources for lanthanides and yttrium, Int. J. Coal Geol. 94 (2012) 67–93.

[9] N. Das, D. Das, Recovery of rare earth metals through biosorption: An overview, J. Rare Earths. 31 (2013) 933–943.

[10] A.A. Korenevsky, V.V. Sorokin, G.I. Karavaiko, Biosorption of rare earth elements, Process Metallurgy. 9 (1999) 299–306.

[11] D. Merten, E. Kothe, G. Büchel, Studies on Microbial Heavy Metal Retention from Uranium Mine Drainage Water with Special Emphasis on Rare Earth Elements, Mine Water Environ. 23 (2004) 34–43.

[12] R.C. Oliveira, O. Garcia Jr., Study of Biosorption of Rare Earth Metals (La, Nd, Eu, Gd) by *Sargassum* sp. Biomass in Batch Systems: Physicochemical Evaluation of

Kinetics and Adsorption Models, Adv. Mater. Res. 71–73 (2009) 605–608.

[13] Ş.□ Sert, C. Kütahyali, S. Inan, Z. Talip, B. Çetinkaya, M. Eral, Biosorption of lanthanum and cerium from aqueous solutions by Platanus orientalis leaf powder, Hydrometallurgy. 90 (2008) 13–18.

[14] V. Diniz, B. Volesky, Biosorption of La, Eu and Yb using Sargassum biomass, Water Res. 39 (2005) 239–247.

[15] J.-A. Barrat, F. Keller, J. Amossé, R. n. Taylor, R. w. Nesbitt, T. Hirata, Determination of Rare Earth Elements in Sixteen Silicate Reference Samples by Icp-Ms After Tm Addition and Ion Exchange Separation, Geostand. Newsl. 20 (1996) 133–139.

[16] W. J. Rourke, W.-C. Lai, S. Natansohn, Ion exchange method for the recovery of scandium, U.S. Patent No. 4,816,233. (28 Mar. 1989).

[17] M.S. Gasser, M.I. Aly, Separation and recovery of rare earth elements from spent nickel-metal-hydride batteries using synthetic adsorbent, Int. J. Miner. Process. 121 (2013) 31–38.

[18] Y. Konishi, J. Shimaoka, S. Asai, Sorption of rare-earth ions on biopolymer gel beads of alginic acid, React. Funct. Polym. 36 (1998) 197–206.

[19] D.S.R. Murty, G. Chakrapani, Preconcentration of rare earth elements on activated carbon and its application to groundwater and sea-water analysis, J. Anal. At. Spectrom. 11 (1996) 815.

[20] R.D. Abreu, C.A. Morais, Purification of rare earth elements from monazite sulphuric acid leach liquor and the production of high-purity ceric oxide, Miner. Eng. 23 (2010) 536–540.

[21] V. Innocenzi, I. De Michelis, F. Ferella, F. Vegliò, Recovery of yttrium from cathode ray tubes and lamps' fluorescent powders: Experimental results and economic simulation, Waste Manag. 33 (2013) 2390–2396.

[22] A. Fakhru'l-Razi, A. Pendashteh, L.C. Abdullah, D.R.A. Biak, S.S. Madaeni, Z.Z. Abidin, Review of technologies for oil and gas produced water treatment, J. Hazard. Mater. 170 (2009) 530–551.

[23] H. Shimizu, K. Ikeda, Y. Kamiyama, Refining of a rare earth including a process for separation by a reverse osmosis membrane, U.S. Patent No. 5,104,544. (14 Apr. 1992).

[24] C. Nakayama, S. Uemiya, T. Kojima, Separation of rare earth metals using a supported liquid membrane with DTPA, J. Alloys Compd. 225 (1995) 288–290.

[25] L. Pei, L. Wang, G. Yu, Study on a novel flat renewal supported liquid membrane with D2EHPA and hydrogen nitrate for neodymium extraction, J. Rare Earths. 30 (2012) 63–68.

[26] B. Wen, X. Shan, S. Xu, Preconcentration of ultratrace rare earth elements in seawater with 8-hydroxyquinoline immobilized polyacrylonitrile hollow fiber membrane for determination by inductively coupled plasma mass spectrometry, Analyst. 124 (1999) 621–626.

[27] Z.V.P. Murthy, M.S. Gaikwad, Separation of praseodymium(III) from aqueous solutions by nanofiltration, Can. Metall. Q. 52 (2013) 7–11.

[28] H.K. Shon, S. Phuntsho, D.S. Chaudhary, S. Vigneswaran, J. Cho, Nanofiltration for water and wastewater treatment - A mini review, Drink. Water Eng. Sci. 6 (2013) 47–53.

[29] N.N. Li, A.G. Fane, W.S.W. Ho, T. Matsuura, Advanced membrane technology and applications, John Wiley & Sons, 2011.

[30] Z. Kovács, W. Samhaber, Characterization of nanofiltration membranes with uncharged solutes, Membrántechnika, 12(2) (2008), 22-36.

[31] C. Aydiner, Y. Kaya, Z.B. Gönder, I. Vergili, Evaluation of membrane fouling and flux decline related with mass transport in nanofiltration of tartrazine solution, J. Chem.

Technol. Biotechnol. 85 (2010) 1229–1240.

[32] W.P. Cathie Lee, S.-K. Mah, C.P. Leo, T.Y. Wu, S.-P. Chai, Phosphorus removal by NF90 membrane: Optimisation using central composite design, J. Taiwan Inst. Chem. Eng. 45 (2014) 1260–1269.

[33] M. Mullett, R. Fornarelli, D. Ralph, Nanofiltration of mine water: Impact of feed pH and membrane charge on resource recovery and water discharge, Membranes (Basel). 4 (2014) 163–180.

[34] K.L. Tu, L.D. Nghiem, A.R. Chivas, Coupling effects of feed solution pH and ionic strength on the rejection of boron by NF/RO membranes, Chem. Eng. J. 168 (2011) 700–706.

[35] J. Tanninen, M. Nyström, Separation of ions in acidic conditions using NF, Desalination. 147 (2002) 295–299.

[36] K. Pickering, M.R. Wiesner, Cost Model for Low-Pressure Membrane Filtration, J. Environ. Eng. 119 (1993) 772–797.

[37] M.R. Wiesner, J. Hackney, S. Sethi, J.G. Jacangelo, J.M. Laine, Cost estimates for membrane filtration and conventional treatment, J. Am. Water Work. Assoc. 86 (1994) 33–41.

[38] S. Chellam, C.A. Serra, M.R. Wiesner, Estimating costs for integrated membrane systems, J. - Am. Water Work. Assoc. 90 (1998) 96–104.

[39] R. Liikanen, J. Yli-Kuivila, J. Tenhunen, R. Laukkanen, Cost and environmental impact of nanofiltration in treating chemically pre-treated surface water, Desalination. 201 (2006) 58–70.

[40] C. Niewersch, C.N. Koh, T. Wintgens, T. Melin, C. Schaum, P. Cornel, Potentials of using nanofiltration to recover phosphorus from sewage sludge, Water Sci. Technol. 57 (2008) 707–714.

[41] I. Vergili, Y. Kaya, U. Sen, Z.B. Gönder, C. Aydiner, Techno-economic analysis of textile dye bath wastewater treatment by integrated membrane processes under the zero liquid discharge approach, Resour. Conserv. Recycl. 58 (2012) 25–35.

[42] T. Lundstedt, E. Seifert, L. Abramo, B. Thelin C Å A, A. Nystrom, J. Pettersen, R. Bergma, Experimental design and optimization, Chemom. Intell. Lab. Syst. 42 (1998) 3–40.

[43] I. Koyuncu, D. Topacik, M.R. Wiesner, Factors influencing flux decline during nanofiltration of solutions containing dyes and salts, Water Res. 38 (2004) 432–440.

[44] S. Sethi, M.R. Wiesner, Simulated cost comparisons of hollow-fiber and integrated nanofiltration configurations, Water Res. 34 (2000) 2589–2597.

[45] S. Sethi, M.R. Wiesner, J. Dennis, Optimization of Hollow-Fiber Design and Low-Pressure Membrane System Operation, J. Environ. Eng. (2001) 485–492.

[46] A. Wahab Mohammad, M. Sobri Takriff, Predicting flux and rejection of multicomponent salts mixture in nanofiltration membranes, Desalination. 157 (2003) 105–111.

[47] S.L. Ong, W.W. Zhou, L.F. Song, W.J. Ng, Evaluation of feed concentration effects on salt/ion transport through RO/NF membranes with the Nernst-Planck-Donnan model, Environ. Eng. Sci. 19 (2002) 429–439.

[48] T. Chidambaram, Y. Oren, M. Noel, Fouling of nanofiltration membranes by dyes during brine recovery from textile dye bath wastewater, Chem. Eng. J. 262 (2015) 156–168.